



# Association of long noncoding RNA MALAT1 with the radiosensitivity of lung adenocarcinoma cells via the miR-140/PD-L1 axis

Shujie Li<sup>a,1</sup>, Yue Xie<sup>a,1</sup>, Wei Zhou<sup>a</sup>, Qian Zhou<sup>a</sup>, Dan Tao<sup>a</sup>, Haonan Yang<sup>b,c</sup>, Kaijin Mao<sup>a</sup>, Shi Li<sup>a</sup>, Jinyan Lei<sup>a</sup>, Yongzhong Wu<sup>a,\*</sup>, Ying Wang<sup>a,2,\*\*</sup>

<sup>a</sup> Radiation Oncology Center, Chongqing University Cancer Hospital & Chongqing Cancer Institute & Chongqing Cancer Hospital, Chongqing, China

<sup>b</sup> College of Bioengineering, Chongqing University, Chongqing, China

<sup>c</sup> School of Medicine, Chongqing University, Chongqing, China

## ARTICLE INFO

### Keywords:

Lung adenocarcinoma  
Long-chain non-coding RNA metastasis-Associated lung adenocarcinoma transcript 1 (lncRNA MALAT1)  
miR-140  
Programmed cell death ligand 1 (PD-L1)  
Catalytic subunit of the DNA-dependent protein kinase (DNA-PKcs)

## ABSTRACT

**Objective:** To investigate the effect of MALAT1 on the modulating the radiosensitivity of lung adenocarcinoma, through regulation of the expression of the miR-140/PD-L1 axis.

**Methods:** The online databases UALCAN and dbDEMC were searched for the MALAT1 and miR-140 expressions in patients with lung adenocarcinoma (LUAD), respectively. Then analyze their relationship with overall survival rates separately in the UALCAN and ONCOMIR databases. A functional analysis was performed for A549 cells by transfecting small-interfering RNAs or corresponding plasmids after radiotherapy. Xenograft models of LUAD exposed to radiation were established to further observe the effects of MALAT1 on the radiosensitivity of LUAD. The luciferase assay and reverse transcription–polymerase chain reaction were performed to assess the interaction between miR-140 and MALAT1 or PD-L1.

**Results:** MALAT1 were overexpressed in human LUAD tumor tissues and cell lines, while miR-140 were inhibited. MALAT1 knockdown or miR-140 increase suppressed cell proliferation and promoted cell apoptosis in LUAD after irradiation. LUAD xenograft tumor growth was also inhibited by MALAT1 knockdown combined with irradiation. miR-140 could directly bind with MALAT1 or PD-L1. Furthermore, MALAT1 knockdown inhibited PD-L1 mRNA and protein expressions by upregulating miR-140 in LUAD cells.

**Conclusion:** MALAT1 may function as a sponge for miR-140a-3p to enhance the PD-L1 expression and decrease the radiosensitivity of LUAD. Our results suggest that MALAT1 might be a promising therapeutic target for the radiotherapy sensitization of LUAD.

## 1. Introduction

Lung cancer is a leading cause of cancer death worldwide, with over 1 million deaths annually [ [1,2]]. Adenocarcinoma is a

\* Corresponding author.

\*\* Corresponding author.

E-mail addresses: [cqmdwyz@163.com](mailto:cqmdwyz@163.com) (Y. Wu), [13996412826@163.com](mailto:13996412826@163.com) (Y. Wang).

<sup>1</sup> Those authors contributed equally.

<sup>2</sup> Lead contact.

<https://doi.org/10.1016/j.heliyon.2023.e16868>

Received 27 November 2022; Received in revised form 27 May 2023; Accepted 31 May 2023

Available online 3 June 2023

2405-8440/© 2023 Published by Elsevier Ltd.

This is an open access article under the CC BY-NC-ND license

(<http://creativecommons.org/licenses/by-nc-nd/4.0/>).

common histopathological type of lung cancer, accounting for approximately 40% of lung cancer cases. Many cases of adenocarcinoma are in the advanced stage at diagnosis. Radiotherapy is a chief therapeutic modality for inoperable, advanced, or metastatic LUAD [3]. Despite technological advances in therapeutic radiotherapy, radioresistance is a roadblock in its effectiveness. Therefore, a better understanding of the molecular mechanisms underlying the radioresistance of LUAD and finding novel predictive biomarkers of radiosensitivity are vital in selecting responsive patients and improving the outcome of radiotherapy.

A number of studies have demonstrated that noncoding RNAs (ncRNAs) are involved in the development, diagnosis, prognosis and treatment of lung cancer [4]. In recent years, ncRNAs were reported to critically participate in CSCs in a variety of cancers [5,6]. The expression patterns of noncoding RNAs (ncRNAs) differ between radiation-resistant and radiation-sensitive tumors after ionizing radiation exposure [7–9]. ncRNAs that are not translated to form a functional protein are involved in diverse biochemical processes. Regulatory ncRNAs can be divided into two categories: long (>200 bp) and small (<200 bp). They include microRNAs (miRNAs), small-interfering RNAs (siRNAs), and piwi-interacting RNAs. Long noncoding RNAs (lncRNAs), with currently a total of over 90,000 annotated genes, can modulate gene expressions and promote the development of different cancer types [10–13].

Metastasis-associated lung adenocarcinoma transcript 1 (MALAT1) was initially found to be overexpressed in non-small cell lung cancer (NSCLC) and considered to be a biomarker for lung cancer metastasis. However, recent studies have reported that MALAT1 is upregulated in various cancer tissues and related to significantly lower overall survival rates in patients with cancer. LncRNA MALAT1 increased the expression of PD-L1 in several cancer cells, and related to significantly lower overall survival rates in patients with cancer. Besides, PD-L1 was modulated by MALAT1 indirectly [4,14]. Overexpression of oncogenic lncRNA MALAT1 promotes the proliferation, invasion, and metastasis of NSCLC. However, little is known about the radioresistance of LUAD or MALAT1.

Many miRNAs have aberrant expressions in various cancers and are involved in oncogenes as well as tumor suppressors. The precursor of miR-140 is located on human chromosome 16. Downregulation of miR-140 promotes the progression of many cancers, including lung cancers, indicating that miR-140 serves as a tumor suppressor. Zhao et al. demonstrated that in NSCLC tissues, the expression level of MALAT1 was negatively correlated with that of miR-200a-3p, while positively correlated with PD-L1. Besides, MALAT1 promoted proliferation, mobility, migration, and invasion of NSCLC cells via sponging miR-200a-3p [14]. Moreover, miR-140 sensitizes cancer cells to radiotherapy [15]. However, the detailed relationship between miR-140 and radioresistance of LUAD remains unclear.

Programmed death 1 ligand 1 (PD-L1), also known as B7–H1 or CD274, is a member of the B7 superfamily that was discovered in 1999. As a negative costimulatory molecule, PD-L1 and its receptor PD-1 can prevent the proliferation and activation of CD4 T cells and CD8 T cells, down regulate the expression of some anti apoptotic molecules and proinflammatory factors, change the tumor micro-environment, weaken the body's ability to monitor and clear tumor cells, and generate immune escape, thus allowing tumor cells to proliferate indefinitely in the body [16]. The aberrantly high PD-L1 expression in most cancers contributes to the low overall survival rate of patients. In addition, most cases of radioresistance to cancers are associated with high PD-L1 expression after irradiation. PD-L1-targeted drugs combined with radiotherapy improve its treatment efficacy for cancer. Overexpression of PD-L1 is a key factor in the radioresistance of tumor cells; however, its molecular mechanism has not been clarified. Currently, little attention has been paid to the effect of lncRNA MALAT1 or miR-140/PD-L1 on irradiated LUAD cells. Therefore, the aim of this study was to investigate how MALAT1/miR-140/PD-L1 regulates the radiosensitivity of LUAD cells.

## 2. Methods and materials

### 2.1. Exploration of genes and miR-RNA expression and survival analysis

UALCAN is an open-access web resource of cancer omics data. We used it to facilitate the discovery of tumors, conduct the normal differential expression analysis of a query gene(s), and obtain the patient survival information based on the gene expression. It originated from The Cancer Genome Atlas datasets [17]. We further evaluated the queried gene expression in cancer and normal tissues using the search function of UALCAN. Subsequently, the boxplot was used to visualize the relationship. Finally, Kaplan–Meier plots were generated by UALCAN to assess the gene prognostic values, and the p-value was calculated.

The database of Differentially Expressed MiRNAs in Human Cancers (dbDEMHC; <https://www.biosino.org/dbDEMC/index>) could provide the integrated information of the miRNA expression in various cancer and normal tissues with high- and low-throughput methods [18]. The dbDEMC 3.0 database was used to investigate the miR-140 expression in patients with LUAD, and all results were downloaded to further obtain a heatmap. In addition, the online ONCOMIR database (<http://www.oncomir.org/>) was used to assess the relationship between the clinical characteristics of patients with LUAD and the alterations in the miRNA expression [19].

### 2.2. Cell culture and RNA interference

All cell lines were purchased from the Cell Bank of Chinese Academy of Sciences (Shanghai, China). The cells were cultured in Dulbecco's Modified Eagle's Medium (DMEM, Gibco, USA), supplemented with 10% fetal bovine serum (FBS, Gibco, USA) and 1% penicillin/streptomycin at 37 °C in a humidified atmosphere of 5% CO<sub>2</sub> atmosphere.

Specific siRNA oligos of MALAT1 and control oligos were synthesized by TSINGKE Co. (Beijing, China). According to the manufacturer's protocol, 50-nM siRNA transfection was performed. The specific siRNA sequences were as follows: MALAT1-specific siRNA-1, 5'-GGCUUUAUCUCAUGAAUCU-3'.

### 2.3. Cell growth assays and cell cycle analyses

Cells in logarithmic growth phase were seeded in 96-well ( $2 \times 10^4$  cells/well). The cell counting kit (CCK-8) reagent (10  $\mu$ l/well; Beyotime, Shanghai, China) was added into each well at 0, 24, 48, 72 and 96 h; the cells were then incubated for another 1 h at 37 °C. The optical density (OD) was assessed under 450-nm wavelength by a microplate reader (Thermo, USA) and normalized to the cell counts.

Cells were seeded onto 6-well plates for 48 h, harvested after washing with phosphate-buffered saline (PBS) twice, fixed with cold 70% ethanol for 20 min, subjected to centrifugation, and washed and resuspended in PBS. They were incubated with 100  $\mu$ l RNase A for 30 min and stained with 400  $\mu$ l propidium iodide for 30 min. Propidium iodide fluorescence was evaluated by Flow Cytometry (CytoFLEX; Beckman, USA).

### 2.4. Colony formation and apoptosis assay

For colony formation assay, A549 cells were seeded into 6-well culture dishes with 100 cells in each well. After 2 weeks of incubation, they were fixed by methanol and then stained with 1 mL of crystal violet for 20 min.

Apoptotic cell death was determined according to AnnexinV-PE/7-AAD (SUNGENE Biotech, China) following manufacturer's instructions. Briefly, the cells were collected, resuspended in binding buffer, stained with Annexin-V-PE Kit and analyzed by flow cytometry in 1 h.

### 2.5. Irradiation of cell line and mice

Male nude mice aged 6–8 weeks and weighted 20–25 g were purchased from Chengdu Dossy Experimental Animal CO., LTD [license no.: SCXK (Chuan) 2020-030]. The specific pathogen-free nude mice were bred at the Western Biotech Technology Co., LTD [license no.: SYXK (Yu) 2019-0002]. Mice were housed at 22–25 °C with a 12-h light/dark cycle and fed with standard chow and water. All mice were sacrificed by anesthesia. The animal protocols were approved by Chongqing university cancer hospital.

We used 96-well plates to inoculate the  $3 \times 10^3$  transfected cell lines/well. A549 cells with MALAT1 shRNA or a nonsense sequence were irradiated by linear accelerator (X-ray, 400Mu/min, VARIAN IX, USA). And cultured for 72 h after the treatment.

The nude mice in this experiments were injected subcutaneously  $1.5 \times 10^6$  cells on each sides of back 10 days before irradiation. Subsequently, they were anesthetized with 7% chloral hydrate, and the back of mice were irradiated by linear accelerator (X-ray, 400Mu/min, VARIAN IX, USA). The tumors were harvested on post-irradiation day 5.

### 2.6. Real-time quantitative polymerase chain reaction (qPCR)

According to the manufacturer's protocol, total RNA was extracted for complementary DNA synthesis using TAKARA kit (TAKARA, JAPAN). The primers for PCR were designed by TSINGKE Co. (Beijing, China) (Table 1). The reverse transcription qPCR conditions were: 95 °C for 5 min; 40 cycles at 95 °C for 10 s and 60 °C for 30s; 95 °C for 15s, 60 °C for 60s and 95 °C for 15s. GAPDH was selected as a reference gene.

### 2.7. Western blot

The extracted protein content was quantified by Bradford protein assay. We separated 36  $\mu$ g of total protein from different cell lines using 10% sodium dodecyl sulfate–polyacrylamide gel electrophoresis and transferred it on a polyvinylidene difluoride membrane. The membrane was blocked by 5% milk and incubated with the diluted primary antibody at 4 °C overnight. Subsequently, it was reacted with horseradish peroxidase-conjugated secondary antibodies at room temperature for 1 h after washing with tris-buffered saline with 0.1% Tween® 20 Detergent for 3 times. The target bands on membrane were detected with ECL plus detection system. The antibodies used for Western blot were: anti-PD-L1 (1:1000, abcam),  $\beta$ -actin (1:1000, HuaBio), anti-rabbit IgG-horseradish peroxidase (1:2000, Beyotime).

**Table 1**  
Gene primer sequence for PCR.

Gene	Primer sequence
MALAT1	(sense) TTAATTGACAGCTGACCCAGGT (antisense) ATCGCACTGGCTCCTGGAC
GAPDH	(sense) AGAAGGCTGGGGCTCATTG (antisense) AGGGCCATCCACAGTCTTC
PD-L1	(sense) CTGAACGCATTTACTGTACAGG (antisense) GAGCTGGTCCTCAACAGCC
U6	(sense) CTCGCTTCGGCAGCAC (antisense) AACGCTTCACGAATTTGCGT
Hsa-mir-140	(sense) GCGGCGGTACCACAGGGTAGAAC (antisense) ATCCAGTGCAGGGTCCGAGG

Immunohistochemical staining of 24 carcinoma tissue samples derived from 12 tumor bearing nude mice was performed with the formalin-fixed paraffin-embedded sections. The sections were deparaffinized with xylene, rehydrated with ethanol, quenched with 3% H<sub>2</sub>O<sub>2</sub> and incubated with PD-L1 or DNA-PKcs antibody at a dilution of 1:100 overnight at 4 °C. After extensive washing in PBS, the sections were further incubated with a secondary antibody for 30 min, visualized with diaminobenzidine as the chromogen, and counterstained with hematoxylin for 5 min. No primary antibody was added in negative control sections. All IHC staining slides were reviewed independently by two experienced pathologists, who were blinded to this study.

## 2.8. Dual luciferase reporter gene

Starbase3.0 was used to predict the binding sites between lncRNA MALAT1 and miR-140. Cells were implanted in 96-well plates and cultured until they grew well. According to the predicted sites, we constructed pmirGLO-MALAT1-wt (including binding sites), pmirGLO-MALAT1-mut (binding site mutation), and pmirGLO as the control group.

Subsequently, the negative control mimics and miR-140 mimics were co-transfected with pmirGLO-MALAT1-wt, pmirGLO-MALAT1-mut, and pmirGLO, respectively. After transfection for 48 h, we removed the culture medium, wash the cells with the PBS, and assessed the luciferase intensity using the dual luciferase reporter system.

## 2.9. Statistical analysis

All statistical analyses were constructed with SPSS 25.0 software. Continuous variables are expressed as mean ± standard deviation. The one-way analysis of variance was performed for between-group differences. Survival curves were plotted with the Kaplan-Meier method and analyzed by the log-rank test. A *p*-value < 0.05 was considered to be statistically significant.

## 3. Results

### 3.1. Expressions of lncRNA MALAT1 and miR-140 in LUAD

To explore the relationship between the expression level and the prognostic value of MALAT1 in patients with LUAD, we used the UALCAN (<http://ualcan.path.uab.edu>). MALAT1 expression levels (*p* = 5.61E-07) were significantly elevated in LUAD cancer tissue than in normal tissue (Fig. 1A). This upregulation (*p* = 0.023) was also related to the significantly poorer overall survival in patients

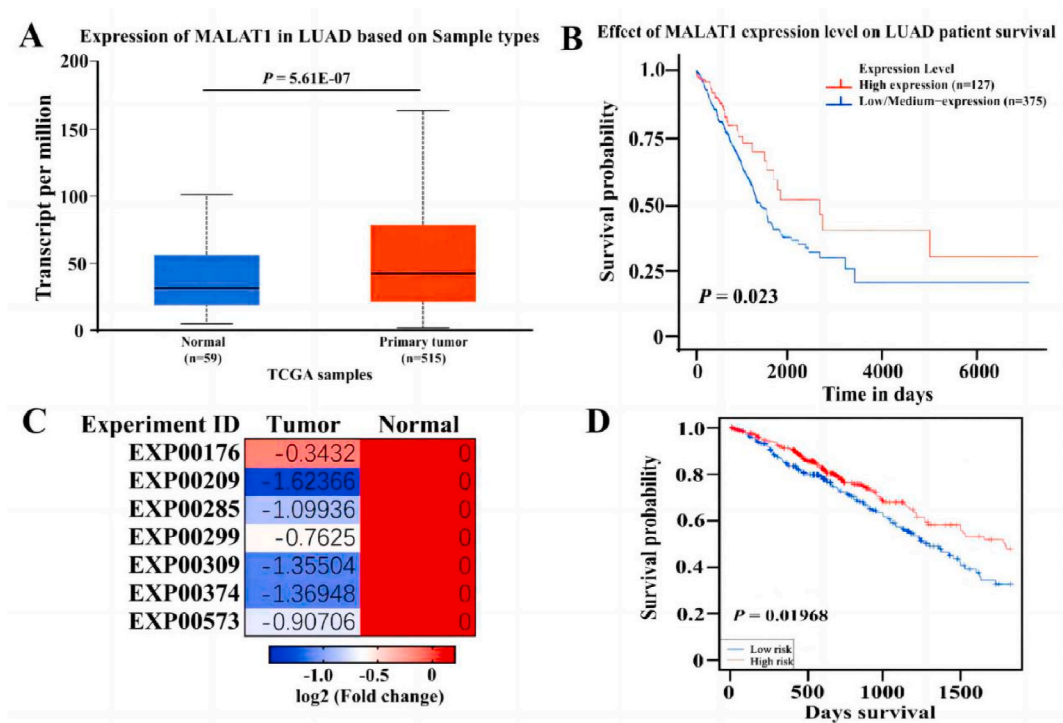


**Fig. 1.** Decreased lncRNA MALAT1A and increased miR-140 are related to the survival of LUAD patients from online database. (A) Upregulated lncRNA MALAT1 was observed in LUAD patients. (B) Relationship between lncRNA MALAT1 and overall survival rate of LUAD patients. (C) Downregulated miR-140 was observed in LUAD patients. (D) Relationship between reduced miR-140 and overall survival rate of LUAD patients; \**p* < 0.05, \*\**p* < 0.01, \*\*\**p* < 0.001. LUAD: lung adenocarcinoma, MALAT1: metastasis-associated lung adenocarcinoma transcript 1.

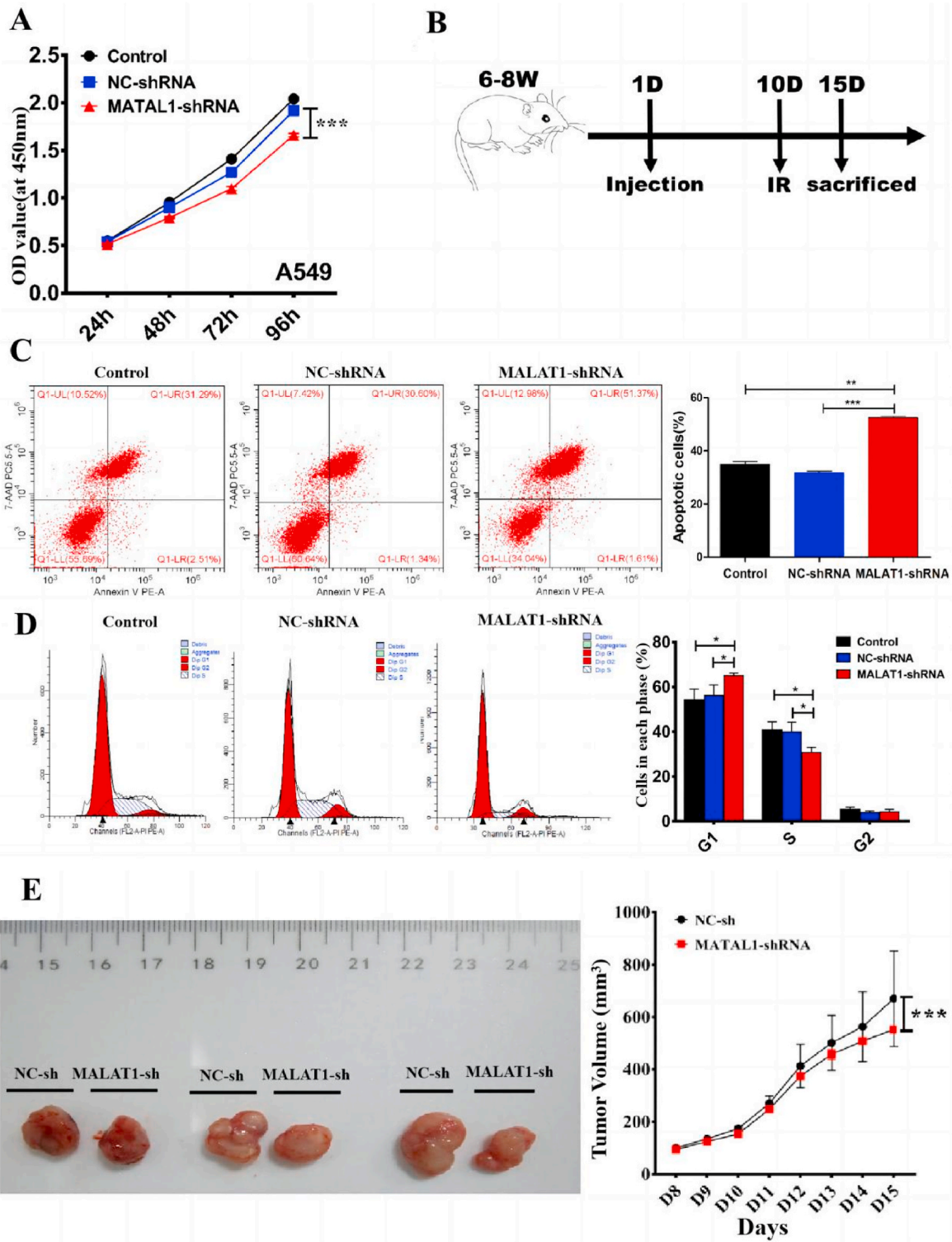


**Fig. 2.** MALAT1 knockdown sensitizes LUAD cells to radiation. (A) The colony-formation assay for the colony survival rate was evaluated in A549 cells transfected with shNC or shMALAT1 under 8 Gy irradiation or radiation therapy alone. (B) The schematic of the establishment of LUAD xenograft mouse model exposed to irradiation. (C) Apoptosis was measured by flow cytometry after transfection in A549 cells. 8Gy + shMALAT1 groups significantly promoted the apoptosis compared with the 8Gy + shNC groups and radiation therapy alone groups in A549. (D) The cell-cycle distribution indicated that the G1/S phase cells were significantly fewer in MALAT1 shRNA +8 Gy groups after irradiation in A549. (E) The tumor growth curve demonstrated that the tumor volume were obviously

small in shMALAT1 combined with radiotherapy groups. Data are presented as mean  $\pm$  SD of three experiments. \* $p < 0.05$ ; \*\* $p < 0.01$ ; \*\*\* $p < 0.001$ . IR: irradiation, PD-L1: programmed cell death ligand 1, NC: normal control, MALAT1: metastasis-associated lung adenocarcinoma transcript 1.

with LUAD (Fig. 1B).

We next utilized the function of the dbDEMCA to obtain the expression of miR-140 in LUAD, and dbDEMCA revealed an evident downregulation of miR-140 in LUAD compared to normal tissues in the seven studies (Fig. 1C). Oncomir indicated that the lower expression of miR-140 ( $p = 0.020$ ) was linked to worse overall survival in patients with LUAD (Fig. 1D).

### 3.2. Association of MALAT1 knockdown with the radiosensitivity of LUAD

To observe the effect of MALAT1 on the radiotherapy of LUAD, human MALAT1 shRNA with stable transfection was constructed. MALAT1 expression reduced in LUAD compared to shRNA of the negative control (shNC) A549 cells. To determine the involvement of MALAT1 in the sensitivity of LUAD cells, CCK-8, colony-formation assay and cell viability assays were performed. After irradiation with 8 Gy, colony-formation assay indicated that combined MALAT1 shRNA and irradiation led to inhibited proliferation of A549 cells compared to shNC with irradiation or radiation therapy alone (Fig. 2A). Moreover, the apoptosis assay demonstrated that MALAT1 shRNA + 8Gy groups had dramatically enhanced apoptosis rates of A549 cells compared to the shNC +8 Gy and radiation therapy alone groups (Fig. 2C). The G1/S phase cells were significantly fewer in the MALAT1 shRNA +8 Gy group than in the shNC +8 Gy group, and the G2 phase cells had no significant difference between the two groups, suggesting that downregulation of the MALAT1 expression has no significant effect on G2 phase cells that increase radiosensitivity (Fig. 2D). These results implied that the downregulation of MALAT1 expression enhanced the radiosensitivity of A549 cell by suppressing cell survival and inducing apoptosis.

To observe the *in vivo* effects of MALAT1 and radiotherapy on tumor growth and survival, we established a A549 cell xenograft mouse model and subcutaneously inoculated the cells transduced with shNC or shMALAT1 into the flanks of nude mice. Ten days later, all mice were irradiated with X-ray at a dose of 6Gy and sacrificed at the five days after radiotherapy. Fig. 2B showed the schematic of the establishment of the LUAD xenograft mouse model exposed to irradiation. Subsequently, the tumor growth curve was measured to calculate the tumor volume. The tumor growth curve showed that the tumor volume at 15 days was significantly lower in the shMALAT1 combined with radiotherapy group than in the shNC combined with radiotherapy group ( $552.34 \pm 8.61 \text{ mm}^3$  vs.  $670.08 \pm 182.19 \text{ mm}^3$   $p < 0.05$ ) (Fig. 2E), indicating that shMALAT1 combined with radiotherapy could inhibit tumor growth effectively.

### 3.3. Association of miR-140 overexpression with the radiosensitivity of LUAD

The miR-140 was correlated with LUAD (Fig. 1C and D). To access the effects of miR-140 on radiosensitivity, we first evaluated miR-140 expression in A549 cells irradiated at a dose of 8Gy. The miR-140 expression was reduced in A549 cells after radiotherapy (Fig. 3A). The miR-140 expression was upregulated to observe its effect on the radiosensitivity of LUAD cells.

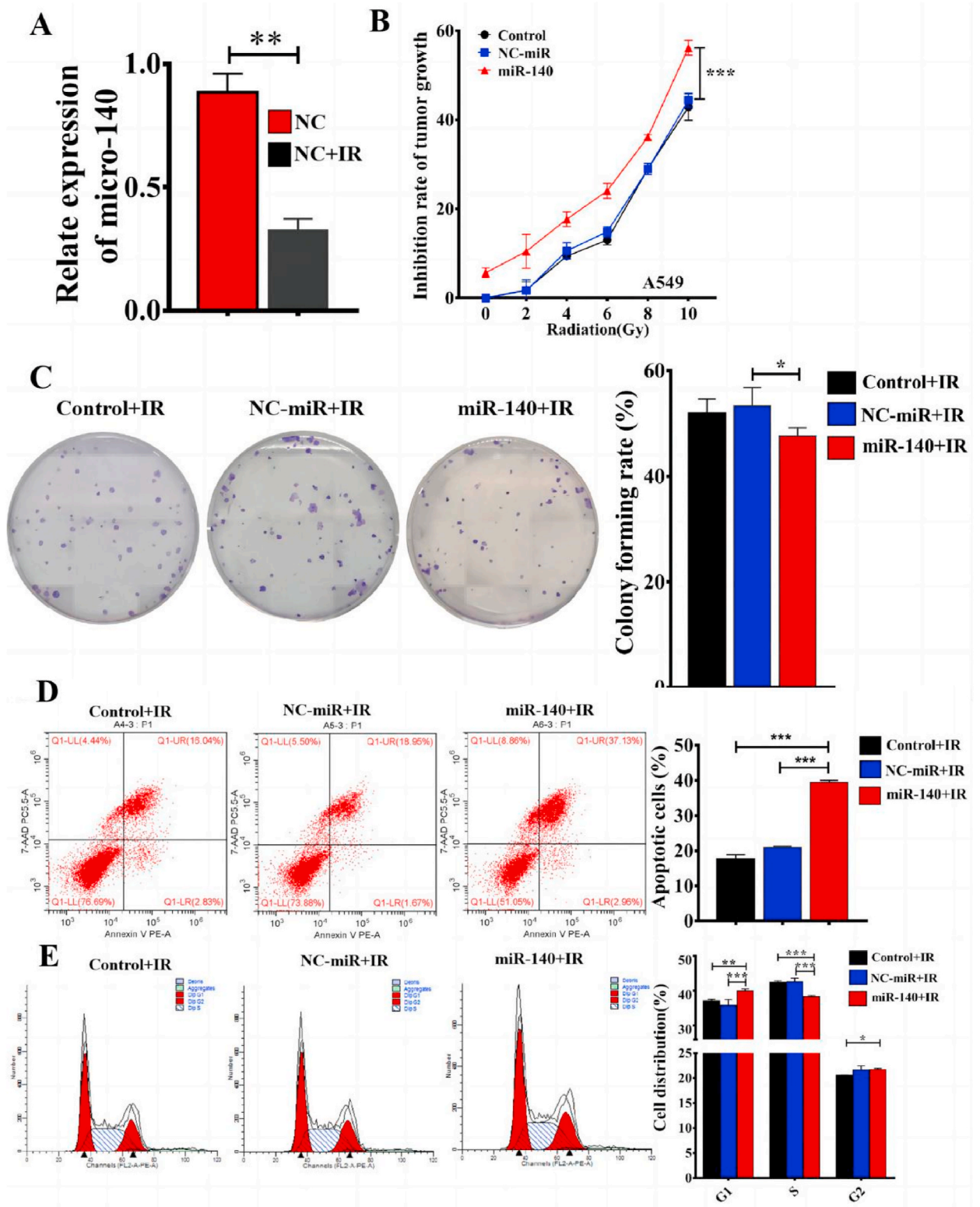
The effect of miR-140 on the radiosensitivity of LUAD was measured by CCK-8. It showed that the effect of miR-140 on LUAD was radiosensitization (Fig. 3B). Upregulated miR-140 combined with 8 Gy radiation suppressed cell proliferation and promote apoptosis (Fig. 3C and D). Furthermore, A549 cells displayed significant S- and G2/M-phase arrest in the miR-140 with 8 Gy radiation group (Fig. 3E). These results suggested that miR-140 inhibited cell survival and enhanced the cell apoptosis and cell-cycle arrest in the irradiated A549 cell lines.

### 3.4. Association of lncRNA MALAT1 with the miR-140 expression

The online database TargetScan was searched to predict which miRNAs would bind with MALAT1. TargetScan revealed an interaction between MALAT1 and miR-140-3p (Fig. 4A). Moreover, MALAT1 knockdown promoted the mRNA expression of miR-140-3p (Fig. 4B). To further verify whether or not miR-140-3p was the direct target of MALAT1, we constructed the WT-MALAT1 luciferase and MUT-MALAT1 reporters. The luciferase intensity has been reduced statistically when WT-MALAT1 was co-transfected with miR-140 mimics (Fig. 4C), suggesting that miR-140-3p can directly target the MALAT1.

### 3.5. Association of MALAT1 knockdown with PD-L1 expression in A549 cells

We examined the expression of PD-L1 and DNA-PKcs (Catalytic subunit of the DNA-dependent protein kinase) in the tissue samples of the xenograft mouse model. Immunohistochemical staining indicated that MALAT1 deficiency significantly restored radiation-induced of PD-L1 and DNA-PKcs overexpressions in the tumor tissue of xenograft mouse model (Fig. 5A), revealing that MALAT1 and PD-L1 may be interrelated in A549 cells after radiotherapy. Moreover, to further verify whether or not MALAT1 regulates PD-L1 expression through miR-140, we detected the mRNA expressions of miR-140 and PD-L1 using reverse transcription-PCR of shMALAT1 and shNC cells after radiotherapy. An upregulated miR-140 expression and a downregulated PD-L1 expression were found in MALAT1-knockdown cells after radiotherapy (Fig. 5B). According to these results, we hypothesized that MALAT1 may plays biological function as a miR-140a-3p sponge to modulate PD-L1 expression. To further find the relationship between PD-L1 and miR-140a-3p, miR-140-3p and negative control mimics were transfected into A549 cells. The miR-140-3p groups showed downregulation of the PD-L1 expression in reverse transcription-PCR (Fig. 5C) and Western blot (Fig. 5D and Fig. S1). To validate whether or not PD-L1 was a direct target of



(caption on next page)

**Fig. 3.** miR-140 sensitized LUAD cells to radiation. (A) The expression of miR-140 was downregulated in A549 cells after the treatment of radiation. (B) CCK-8 assay for cell growth vitality was performed in A549 cells transfected with miR-140-3p mimics or miR-140-3p NC with different doses of irradiation. (C) The colony-formation assay for the colony survival rate was evaluated in A549 cells transfected with miR-140-3p mimics or miR-140-3p NC under 8 Gy irradiation or radiation therapy alone. (D) Apoptosis was measured by flow cytometry after transfection in A549 cells. 8Gy + miR-140 NC groups significantly promoted the apoptosis compared with the 8Gy + miR-140-3p mimics groups and radiation therapy alone groups in A549. (E) The cell-cycle distribution indicated that the G2/M phase cells were significantly fewer in 8Gy + miR-140 NC groups after irradiation in A549. Data are presented as mean  $\pm$  SD of three experiments. \* $p < 0.05$ ; \*\* $p < 0.01$ ; \*\*\* $p < 0.001$ . IR: irradiation, NC: normal control.

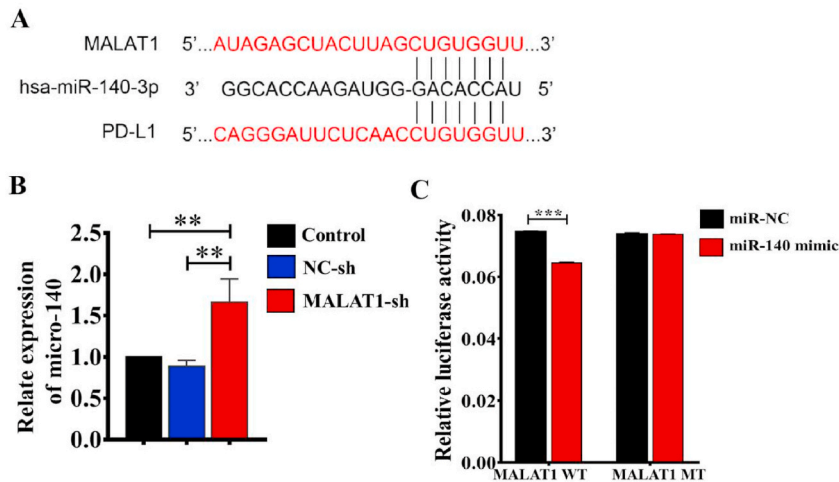


**Fig. 4.** lncRNA MALAT1 modulates the expression of miR-140 by directly binds in A549 cells. (A) Schematic of MALAT1 3'UTR luciferase reporter vector. (B) The expression of miR-140 was downregulated in MALAT1 knockdown cells after the treatment of radiation. (C) The relative luciferase activities were evaluated in A549 cells cotransfected with miR-140-3p or miR-140-3p NC. Data are presented as mean  $\pm$  SD of three experiments. \* $p < 0.05$ ; \*\* $p < 0.01$ ; \*\*\* $p < 0.001$ . PD-L1: programmed cell death ligand 1, NC: normal control, MALAT1: metastasis-associated lung adenocarcinoma transcript 1. WT: wild type, MT: mutation type.

miR-140a-3p, wild-type (WT) PD-L1 or mutant 3'-UTR (MUT) PD-L1 were co-transfected into cells with miR-140 or negative control mimics in a luciferase reporter assay. This results showed that miR-140a-3p mimics significantly reduced the luciferase activity of WT PD-L1 compared to the negative control group, while the luciferase activity of MUT- PD-L1 in A549 cells showed no differences (Fig. 5E).

#### 4. Discussion

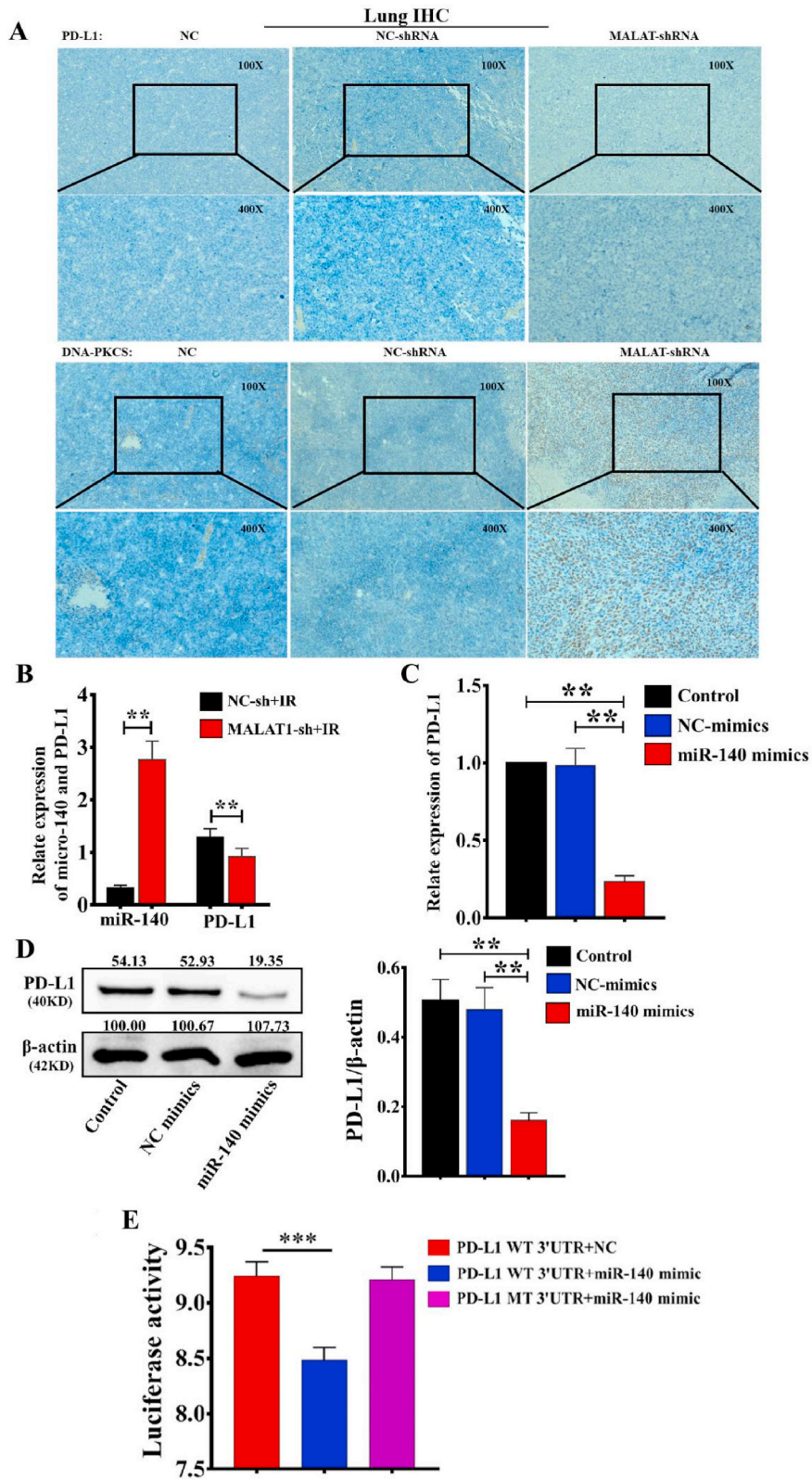
Radiotherapy is a chief therapeutic for cancer that is widely used for inoperable cancers, such as advanced lung cancer [3,20]. Some lncRNA might be key regulators of the radioresistance of LUAD [21,22]. The lncRNA MALAT1 has been implicated in the development of various cancers. However, its role in the radioresistance of LUAD with potential mechanisms have not been fully illustrated. The aim of this study was to investigate the regulatory function role of MALAT1 in the radiosensitivity of LUAD.

According to the results of the online database, compared with non-cancerous tissues, LUAD tissues showed increased expression of MALAT1 and decreased expression of miR-140. Similar expression trends of lncRNA MALAT1 and miR-140 were observed in cells, consistent with previous reports [23,24]. In additions, the overall survival time of the downregulated MALAT1 and upregulated miR-140 groups was markedly better compared to upregulated MALAT1 and downregulated miR-140 groups, respectively. Taken together, these data indicated that lncRNA MALAT1 and miR-140 might be related to LUAD.

In this study, MALAT1 knockdown inhibited malignant proliferation and colony formation and promoted apoptosis and cell-cycle arrest in irradiated LUAD cells. The LUAD xenograft mouse model treated with radiation showed similar results. In addition, miRNAs regulate radiosensitivity by interacting with the vital radiation-related genes in tumor cells [25,26]. However, whether or not the miR-140 expression affects radiosensitivity in cancers is unknown.

In our study, miR-140 increased cell proliferation and colony formation and inhibited apoptosis and cell-cycle G2 arrest in irradiated LUAD cells. Since the G2/M phase is the most radiosensitive phase, activated G2/M arrest can stop cell-cycle progression, allowing time for DNA double-strand breaks to repair and help the tumor cells survive. These data suggested that both MALAT1 and miR-140 regulated the radiosensitivity of LUAD. Based on these results, we hypothesized that there is an association between MALAT1 and miR-140. TargetScan revealed that MALAT1 had a binding site with the miR-140. This interaction between MALAT1 and miR-140 was confirmed using the luciferase reporter assay. These data supported the hypothesis that MALAT1 and miR-140 had a direct interaction in LUAD cells.

To find the downstream target genes of lncRNA MALAT1/miR-140 regulatory axis, we further performed the IHC to observe the



(caption on next page)

**Fig. 5.** MALAT1 knockdown regulates PD-L1 expression via miR-140 in A549 cells. (A) PD-L1 and DNA-PKcs staining of tumor tissue from LUAD xenograft mouse model treated with radiation. (B) Upregulated miR-140-3p expression and downregulated PD-L1 expression in shMALAT1 cells. (C) The downregulated PD-L1 mRNA expression in miR-140 cells. (D) The downregulated PD-L1 protein expression in miR-140 cells. (E) Schematic of PD-L1 3'UTR wild-type (WT) and mutant (MT) luciferase reporter vector. The relative luciferase activities were evaluated in A549 cells cotransfected with miR-140-3p or miR-140-3p NC. Data are presented as mean  $\pm$  SD of three experiments. \* $p < 0.05$ ; \*\* $p < 0.01$ ; \*\*\* $p < 0.001$ . IR: irradiation, PD-L1: programmed cell death ligand 1, DNA-PKcs: Catalytic subunit of the DNA-dependent protein kinase. NC: normal control, MALAT1: metastasis-associated lung adenocarcinoma transcript 1.

PD-L1 expression in the tumor tissue from the LUAD xenograft mouse model after irradiation. MALAT1 knockdown reduce the PD-L1 expression in the xenograft mouse model after irradiation. Additionally, Ji et al. showed that miR-140 negatively correlated with the PD-L1 expression in osteosarcoma cells and directly regulated it in the luciferase reporter gene assay, thereby increasing the infiltration of cytotoxic CD8 + T cells and inhibiting tumor growth in immune-active C57BL/6J mice [27]. Therefore, we hypothesized that MALAT1 plays biological function as a miR-140a-3p sponge to modulate PD-L1 expression. We further presented that transfection of miR-140a-3p into A549 cells significantly reduced the PD-L1 expression. We also confirm the direct binding of miR-140a-3p to PD-L1 using the dual luciferase reporter gene assay. These findings showed that there is a negative relationship between the miR-140 and PD-L1 expression, thus suppressing the immune escape of tumor cells.

This study experimented the expression of PD-L1 and miR-140 after MALAT1 knockdown in lung adenocarcinoma A549 cells, as well as the miR-140 sensitized LUAD cells to radiation, and investigated the negative relationship between PD-L1 and miR-140 expression. However, there hasn't investigated the specific interaction mechanism between MALAT1 and miR-140. Besides, after the change in PD-L1 expression, further verification of the immune status and T cell changes in nude mice can reflect changes in the body's immune function, and better verify the radiation regulatory effect of miR-140/PD-L1 axis in the model body. Those are the limitations of this study, we looking forward to further confirmation through subsequent experiments.

## 5. Conclusion

The findings of this study indicate that MALAT1 knockdown promotes the radiosensitivity of LUAD by regulating the miR-140/PD-L1 axis. Targeting the MALAT1 miR-140/PD-L1 axis might represent a novel therapeutic application to the radiosensitivity of LUAD.

## Author contributions

Shujie Li; Yue Xie: Conceived and designed the experiments; Analyzed and interpreted the data; Contributed reagents, materials, analysis tools or data; Wrote the paper.

Dan Tao: Conceived and designed the experiments.

Ying Wang; Yongzhong Wu: Conceived and designed the experiments; Contributed reagents, materials, analysis tools or data.

Qian Zhou: Performed the experiments; Analyzed and interpreted the data; Contributed reagents, materials, analysis tools or data; Wrote the paper.

Wei Zhou; Haonan Yang; Kaijin Mao; Shi Li; Jinyan Lei: Performed the experiments.

## Data availability statement

Data included in article/supp. material/referenced in article.

## Declaration of competing interest

The authors declare that the research was conducted in the absence of any commercial or financial relationships that could be construed as a potential conflict of interest. All authors have read and concurred with the content of the manuscript.

## Appendix A. Supplementary data

Supplementary data to this article can be found online at <https://doi.org/10.1016/j.heliyon.2023.e16868>.

## References

- [1] F. Bray, J. Ferlay, I. Soerjomataram, R.L. Siegel, L.A. Torre, A. Jemal, Global cancer statistics 2018: GLOBOCAN estimates of incidence and mortality worldwide for 36 cancers in 185 countries, *CA Cancer J Clin* 68 (6) (2018) 394–424, <https://doi.org/10.3322/caac.21492>.
- [2] R.L. Siegel, K.D. Miller, A. Jemal, Cancer statistics, 2020, *CA Cancer J Clin* 70 (1) (2020) 7–30, <https://doi.org/10.1016/j.neo.2017.05.002>.
- [3] S. Tyldesley, C. Boyd, K. Schulze, H. Walker, W.J. Mackillop, Estimating the need for radiotherapy for lung cancer: an evidence-based, epidemiologic approach, *Int. J. Radiat. Oncol. Biol. Phys.* 49 (4) (2001) 973–985, <https://doi.org/10.1007/s11356-021-12509-5>.
- [4] S. Wei, K. Wang, X. Huang, Z. Zhao, Z. Zhao, LncRNA MALAT1 contributes to non-small cell lung cancer progression via modulating miR-200a-3p/programmed death-ligand 1 axis, *Int. J. Immunopathol. Pharmacol.* 33 (2019), 2058738419859699, <https://doi.org/10.1093/nar/gkx1107>.

- [5] J. Melendez-Zajgla, V. Maldonado, The role of lncRNAs in the stem phenotype of pancreatic ductal adenocarcinoma, *Int. J. Mol. Sci.* 22 (12) (2021), <https://doi.org/10.21873/anticancer.11825>.
- [6] B. Humphries, Z. Wang, C. Yang, MicroRNA regulation of breast cancer stemness, *Int. J. Mol. Sci.* 22 (7) (2021), <https://doi.org/10.1016/j.omtn.2020.09.020>.
- [7] G. Li, Y. Liu, C. Liu, Z. Su, S. Ren, Y. Wang, T. Deng, D. Huang, Y. Tian, Y. Qiu, Genome-wide analyses of long noncoding RNA expression profiles correlated with radioresistance in nasopharyngeal carcinoma via next-generation deep sequencing, *BMC Cancer* 16 (1) (2016) 719, <https://doi.org/10.3390/ijms22073756>.
- [8] J. Zhou, S. Cao, W. Li, D. Wei, Z. Wang, G. Li, X. Pan, D. Lei, Time-course differential lncRNA and mRNA expressions in radioresistant hypopharyngeal cancer cells, *Oncotarget* 8 (25) (2017) 40994–41010, <https://doi.org/10.1016/j.bbrc.2017.11.120>.
- [9] D. Yu, Y. Li, Z. Ming, H. Wang, Z. Dong, L. Qiu, T. Wang, Comprehensive circular RNA expression profile in radiation-treated HeLa cells and analysis of radioresistance-related circRNAs, *PeerJ* 6 (2018), e5011, <https://doi.org/10.7717/peerj.5011>.
- [10] S. Fang, L. Zhang, J. Guo, Y. Niu, Y. Wu, H. Li, L. Zhao, X. Li, X. Teng, X. Sun, et al., NONCODEV5: a comprehensive annotation database for long non-coding RNAs, *Nucleic Acids Res.* 46 (D1) (2018) D308–D314, <https://doi.org/10.1016/j.canrad.2011.05.001>.
- [11] Q. Zhou, X. Tang, X. Tian, J. Tian, Y. Zhang, J. Ma, H. Xu, S. Wang, lncRNA MALAT1 negatively regulates MDSCs in patients with lung cancer, *J. Cancer* 9 (14) (2018) 2436–2442, <https://doi.org/10.1186/s12885-016-2755-6>.
- [12] L. Lin, H. Li, Y. Zhu, S. He, H. Ge, Expression of metastasis-associated lung adenocarcinoma transcript 1 long non-coding RNA in vitro and in patients with non-small cell lung cancer, *Oncol. Lett.* 15 (6) (2018) 9443–9449, <https://doi.org/10.3892/ol.2018.8531>.
- [13] Y. Jin, S.J. Feng, S. Qiu, N. Shao, J.H. Zheng, lncRNA MALAT1 promotes proliferation and metastasis in epithelial ovarian cancer via the PI3K-AKT pathway, *Eur. Rev. Med. Pharmacol. Sci.* 21 (14) (2017) 3176–3184, <https://doi.org/10.3390/ijms22126374>.
- [14] Z. Song, X. Wang, F. Chen, Q. Chen, W. Liu, X. Yang, X. Zhu, X. Liu, P. Wang, lncRNA MALAT1 regulates METTL3-mediated PD-L1 expression and immune infiltrates in pancreatic cancer, *Front. Oncol.* 12 (2022), 1004212, <https://doi.org/10.3390/cancers12061662>.
- [15] V. Flamini, W.G. Jiang, Y. Cui, Therapeutic role of MiR-140-5p for the treatment of non-small cell lung cancer, *Anticancer Res.* 37 (8) (2017) 4319–4327, <https://doi.org/10.3322/caac.21708>.
- [16] R.A. Wilcox, A.L. Feldman, D.A. Wada, Z.Z. Yang, N.I. Comfere, H. Dong, E.D. Kwon, A.J. Novak, S.N. Markovic, M.R. Pittelkow, et al., B7-H1 (PD-L1, CD274) suppresses host immunity in T-cell lymphoproliferative disorders, *Blood* 114 (10) (2009) 2149–2158, <https://doi.org/10.1182/blood-2009-04-216671>.
- [17] D.S. Chandrashekar, B. Bashel, S.A.H. Balasubramanya, C.J. Creighton, I. Ponce-Rodriguez, B. Chakravarthi, S. Varambally, UALCAN: a portal for facilitating tumor subgroup gene expression and survival analyses, *Neoplasia* 19 (8) (2017) 649–658, <https://doi.org/10.3389/fonc.2022.1004212>.
- [18] Z. Yang, L. Wu, A. Wang, W. Tang, Y. Zhao, H. Zhao, A.E. Teschendorff, dbDEM2.0: updated database of differentially expressed miRNAs in human cancers, *Nucleic Acids Res.* 45 (D1) (2017) D812–D818, [https://doi.org/10.1016/s0360-3016\(00\)01401-2](https://doi.org/10.1016/s0360-3016(00)01401-2).
- [19] N.W. Wong, Y. Chen, S. Chen, X. Wang, OncomiR: an online resource for exploring pan-cancer microRNA dysregulation, *Bioinformatics* 34 (4) (2018) 713–715, <https://doi.org/10.1177/2058738419859699>.
- [20] A. Joubert, G. Vogin, C. Devic, A. Granzotto, M. Viau, M. Maalouf, C. Thomas, C. Colin, N. Foray, [Radiation biology: major advances and perspectives for radiotherapy], *Cancer Radiother.* 15 (5) (2011) 348–354, <https://doi.org/10.1093/bioinformatics/btx627>.
- [21] F. Han, S. Yang, W. Wang, X. Huang, D. Huang, S. Chen, Silencing of lncRNA LINC00857 enhances BIRC5-dependent radio-sensitivity of lung adenocarcinoma cells by recruiting NF- $\kappa$ B1, *Mol. Ther. Nucleic Acids* 22 (2020) 981–993, <https://doi.org/10.1093/nar/gkw1079>.
- [22] M. Zhang, C. Gao, Y. Yang, G. Li, J. Dong, Y. Ai, N. Chen, W. Li, Long noncoding RNA CRNDE/PRC2 participated in the radiotherapy resistance of human lung adenocarcinoma through targeting p21 expression, *Oncol. Res.* 26 (8) (2018) 1245–1255, <https://doi.org/10.7717/peerj.5011>.
- [23] J. Zhang, M. Wang, J. Wang, W. Wang, JMJD2C-mediated long non-coding RNA MALAT1/microRNA-503-5p/SEPT2 axis worsens non-small cell lung cancer, *Cell Death Dis.* 13 (1) (2022) 65, <https://doi.org/10.1371/journal.pone.0073604>.
- [24] Y. Yuan, Y. Shen, L. Xue, H. Fan, miR-140 suppresses tumor growth and metastasis of non-small cell lung cancer by targeting insulin-like growth factor 1 receptor, *PLoS One* 8 (9) (2013), e73604, <https://doi.org/10.1038/s41419-022-04513-5>.
- [25] Y. Chen, J. Cui, Y. Gong, S. Wei, Y. Wei, L. Yi, MicroRNA: a novel implication for damage and protection against ionizing radiation, *Environ. Sci. Pollut. Res. Int.* 28 (13) (2021) 15584–15596, <https://doi.org/10.3727/096504017x14944585873668>.
- [26] M. Podralska, S. Ciesielska, J. Kluiwer, A. van den Berg, A. Dzikiewicz-Krawczyk, I. Slezak-Prochazka, Non-Coding RNAs in cancer radiosensitivity: MicroRNAs and lncRNAs as regulators of radiation-induced signaling pathways, *Cancers* 12 (6) (2020), <https://doi.org/10.18632/oncotarget.17343>.
- [27] X. Ji, E. Wang, F. Tian, MicroRNA-140 suppresses osteosarcoma tumor growth by enhancing anti-tumor immune response and blocking mTOR signaling, *Biochem. Biophys. Res. Commun.* 495 (1) (2018) 1342–1348, <https://doi.org/10.7150/jca.24796>.